INTERNATIONAL UNION OF PURE
AND APPLIED CHEMISTRY

MACROMOLECULAR DIVISION
COMMISSION ON POLYMER CHARACTERIZATION AND PROPERTIES
WORKING PARTY ON STRUCTURE AND PROPERTIES OF COMMERCIAL POLYMERS*

STUDIES ON BIODEGRADABLE POLY(HEXANO-6-LACTONE) FIBERS 1. STRUCTURE AND PROPERTIES OF DRAWN POLY(HEXANO-6-LACTONE) FIBERS

(Technical Report)

Prepared for publication by
MASATSUGU MOCHIZUKI[1], KAZUO NAKAYAMA[2], RENYUAN QIAN[3],
BING-ZHENG JIANG[4], MATSUO HIRAMI[1], TOSHIO HAYASHI[5], TOSHIRO MASUDA[6]
AND AKIO NAKAJIMA[7]

[1]Research and Development Center, Unitika Ltd., 23, Uji-Kozakura, Uji, Kyoto 611, Japan
[2]National Institute of Materials and Chemical Research, Tsukuba, Ibaraki 305, Japan
[3]Institute of Chemistry, Academia Sinica, Beijing 100080, China
[4]Changchun Institute of Applied Chemistry, Academia Sinica, Changchun, Jilin, China
[5]Research Institute for Advanced Science and Technology, Osaka Prefecture University, Sakai, Osaka 593, Japan
[6]Department of Material Chemistry, Kyoto University, Yoshida, Sakyou-ku, Kyoto 606-01, Japan
[7]4-1-5 Midoridai, Kawanishi, Hyogo 666-01, Japan

Studies on biodegradable poly(hexano-6-lactone) fibers 1. Structure and properties of drawn poly(hexano-6-lactone) fibers (Technical Report)

Synopsis : Using high molecular weight (M_n=80,000) Poly(hexano-6-lactone) (PCL*), tough and high tenacity PCL monofilaments with various draw ratios (undrawn to 9 times drawn) were prepared by melt-spinning. The relationship between microstructure and properties of the PCL fibers is described in this current IUPAC Technical Report. Analysis of microstructure of the drawn PCL fibers by wide-angle X-ray diffraction revealed typical c-axis orientation with an increase in crystallinity. It was also supported by sonic velocity measurements. The thermal, mechanical, and dynamic mechanical properties of the PCL fibers were affected significantly by draw ratio. DSC thermograms showed that the melting temperature and the enthalpy of fusion increased with draw ratio. The temperature dependence curves of dynamic viscoelasticity showed that the temperature at $\tan \delta$ peak of α dispersion corresponding to the glass transition temperature shifted toward higher temperature and the peak value of $\tan \delta$ decreased with draw ratio. The dynamic storage modulus and the sonic modulus increased with draw ratio. These results are due to the increase in crystallinity and molecular orientation with drawing, and are responsible for an increase in tensile tenacity as well as knot tenacity of the PCL fibers.

INTRODUCTION

Environmental pollutions brought about by plastic wastes have become a global problem. One of the solutions to the problem on plastic wastes is an application of biodegradable thermoplastics which degrade in soil, sea or lake water, activated sludge, and compost after their service life has been over.

Bioabsorbable sutures from polyglycolide and their copolymers that decompose *in vivo* by chemical hydrolysis, have been well known since 25 years ago as applications of biodegradable thermoplastics to fibers or nonwovens. However, the materials are sensitive to moisture and lead to hydrolysis in humid atmospheres without humidity-proof packaging. Environmentally degradable man-made fibers (ref. 1) for commodity or industrial uses such as disposable products or agricultural materials, should be resistant to chemical hydrolysis in humid atmosphere and be primarily degraded by enzymes secreted by microorganisms in compost, soil, water, and activated sludge.

Poly(hexano-6-lactone) (PCL*) is an aliphatic polyester that is relatively stable synthetic polymer under a usual condition and is biodegradable under microbial attack. PCL is a partially crystalline polymer that has a moderately low melting point of 60 °C. The polymer can be melt spun to exhibit a tough and high-strength fiber. There has been, however, little study on its fiber-making, probably because of the relatively low melting point.

PCL fibers have been manufactured by a melt-spinning process with subsequent drawing. The relationship between structure and properties of the PCL fibers with various draw ratios is described in the present study. The environmental degradation behaviour of the PCL fibers in soil and in water will be described in the second IUPAC Technical Report and the effect of morphology on enzymatic degradation will be discussed in detail in the third IUPAC Technical Report.

---

*The name' ε -caprolactone' is commonly used rather that the IUPAC nomenclature 'hexano-6-lactone'; hence the abbreviation PCL, based on the former, is used throughout this Technical Report.
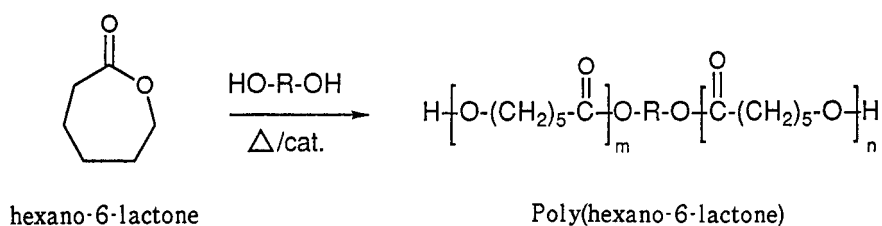
Fig. 1. Synthesis scheme of poly(hexano-6-lactone)

EXPERIMENTAL

Materials

PCL is a linear aliphatic polyester resin prepared through the ring opening polymerization of hexano-6-lactone as shown in Figure 1 (ref. 2). The cyclic ester monomer will open in the presence of an initiator that contains an active hydrogen atom. Although the polymerization will proceed without a catalyst, the reaction is greatly facilitated by catalysts such as stannous octanoate. When a diol (HO-R-OH, where R = aliphatic segment) like diethylene glycol is used as the initiator, a dihydroxy-terminated polymer is formed. It exhibits a reduced tendency to hydrolyze, compared to conventional polyesters, since residual carboxylic acid end groups are basically absent.

The PCL polymer is available from Union Carbide Corporation in the trade name of TONE. TONE P-787 is a tough, extensible polymer with the number-average molecular weight (M_n) of about 80,000, and consequently it was used to prepare a high tenacity fiber. The basic physical properties of TONE P-787 are shown in Table 1 (ref. 3). It is a semi-rigid material at room temperature with an modulus between those of low-density and high-density polyethylenes.

Preparation of fibers

Tough and high tenacity PCL monofilaments of TONE P-787 were prepared by melt-spinning at 210°C. The monofilaments were manufactured by the so-called spin-draw process in which as-spun yarns were immediately introduced into water bath at 25°C for quenching, then passed to drawing zones at room temperature to 45°C, and subsequently passed to a relaxing zone. Monofilaments with almost the same diameters (280 ± 5 μ m) and different draw ratios (undrawn to 9 times drawn) were prepared.

Measurements of densities

Densities of PCL fibers were measured by a density gradient column of NaCl aqueous solution at 20 ± 1°C. Short-cut PCL fibers were immersed in ethanol anhydride solution under reduced pressure for more than ten minutes in order to degas before putting them into the density gradient column. After four hours flotation, densities were calculated from the calibration curve by standard floats.

Thermal analysis

The melting temperature (T_m) of PCL fibers was recorded on a differential scanning calorimeter (DSC), Perkin-Elmer DSC-7, at a heating rate of 20°C/min. T_m and the enthalpy of fusion (ΔH_m) were determined from the DSC endotherms.

Table 1. Basic properties of PCL

Trade name/Grade	Tone/P-787
Number-average molecular weight: M_n	80,000
Melting point: T_m (°C)	60
Glass transition temperature: T_g (°C)	−60

Tensile and knot tests

Using a tensile testing machine, Autograph S-100 (Shimadzu Co.), tensile and knot properties of PCL fibers were measured in accordance with a standard method, JIS L-1013. A crosshead speed of 30 cm/min and a gauge length of 25 cm were used for drawn fibers, and a crosshead speed of 10 cm/min and a gauge length of 2 cm were used for undrawn fibers.

Measurement of dynamic viscoelasticity

Dynamic viscoelastic properties of PCL fibers were measured as a function of temperature by a non-resonant forced-vibration type apparatus, Rheovibron DDV-II-EP (Orientec) at the heating rate of 1°C/min. The measuring frequencies were selected at 3.5, 11, 35, and 110 Hz. The dynamic strain of 4×10^{-4} was applied.

X-ray diffraction

Microstructures of PCL fibers were evaluated by wide-angle X-ray diffraction (WAXD). WAXD diagrams of the samples were recorded by using CuK α radiation with RAD-C (Rigaku Denki Co. Ltd.). WAXD profiles were obtained in the range of $2\theta = 5$ to $125°$. Crystallinity was evaluated by WAXD using the Ruland method (ref. 4). The degree of orientation of drawn PCL fibers was evaluated by Hermans orientation function (ref. 5,6) calculated from the azimuthal intensity profile along the diffraction ring of (006).

Measurement of sonic velocity

The velocity of longitudinal wave in PCL fibers was determined by measuring the transit time of a sonic pulse at a frequency of 1.33kHz and 10kHz. The measurements were conducted at 23°C. The length of specimen between the transmitting and receiving transducers was varied from 150 to 250mm.

RESULTS AND DISCUSSION

Thermal, mechanical, and thermo-mechanical properties

Thermo-mechanical properties of the fibers are important in relation to their application. The thermal, mechanical, and dynamic mechanical properties of PCL fibers were affected significantly by draw ratio (DR). Figure 2 shows DSC thermograms of PCL fibers with various draw ratios.
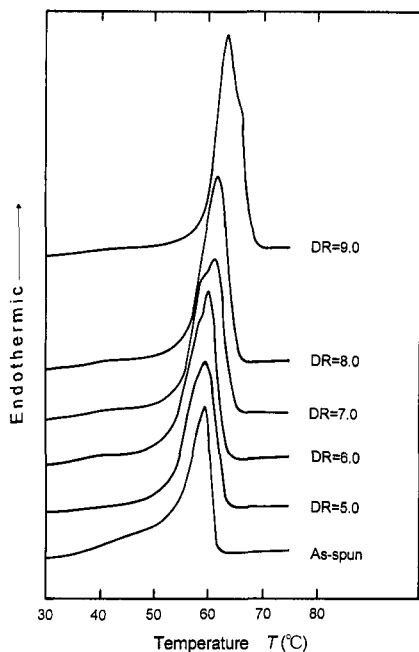

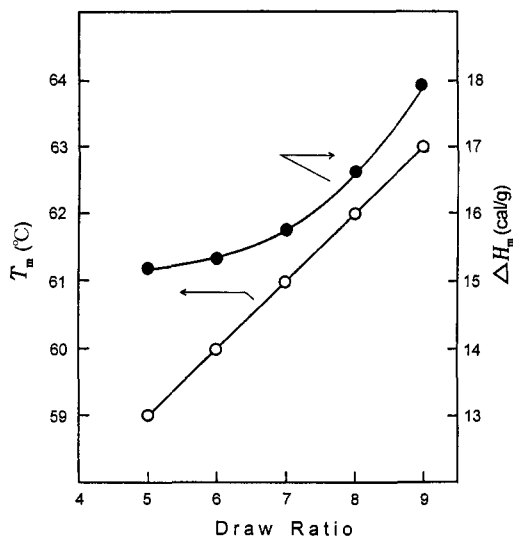Fig. 2. DSC thermograms of PCL fibers with various draw ratios.

Fig. 3. Effects of draw ratio on melting temperature, T_m, and enthalpy of fusion, $\triangle H_m$.

Table 2. Thermal properties and crystalline phase parameters of PCL fibers

Draw Ratio	Density (g/cm3)	T_m (°C)	ΔH_m (cal/g)	Degree of Orientation (%)	Crystallinity Index (%)
DR=1 (undrawn)	1.1403	59	15.8	0.3368	40.0
DR=5 (drawn)	1.1438	60	15.2	0.9684	63.3
DR=6 (drawn)	1.1443	61	15.3	0.9698	63.3
DR=7 (drawn)	1.1446	62	15.7	0.9767	65.0
DR=8 (drawn)	1.1463	63	16.6	0.9820	66.7
DR=9 (drawn)	1.1484	64	17.9	0.9886	69.3

The melting temperature (T_m) and the enthalpy of fusion (ΔH_m) are shown in Table 2 and are plotted as functions of draw ratio in Figure 3. T_m increases linearly from 59 to 64°C with draw ratio, and ΔH_m increases slowly at low DR and rapidly at high DR with drawing. These results imply that the size of crystallites and the crystallinity increase with drawing.

Tensile properties of PCL fibers are plotted against draw ratio in Figure 4(a). The results obtained in the figure indicate that tensile tenacity increases with an increase in draw ratio, reaching more than 8 g/d at DR=9. The behavior of ultimate elongation is contrast to it. These results are generally observed, and are due to an increase in molecular orientation along the fiber axis with increasing crystallinity by drawing. An effect of draw ratio on knot properties is similar to that of the tensile properties as shown in Figure 4(b).

Figure 5 shows the curves of temperature dependence of dynamic mechanical properties of PCL fibers, measured by use of non-resonant forced-vibration method. The $\tan \delta$ curve for undrawn PCL fiber demonstrates two loss peaks which are attributed to the α and β dispersions of PCL at -60 and -125°C, respectively. The α dispersion corresponds to the glass transition of the material. The temperature at $\tan \delta$ peak of α dispersion is shifted toward higher temperatures with an increase in draw ratio. On the other hand, the temperature at β transition peak is almost constant.

To see more precisely the change of glass transition temperature (T_g) with drawing, the temperatures at $\tan \delta$ peak are plotted against draw ratio as shown in Figure 6. It is clear that the T_g increases significantly with the increase in draw ratio. This suggests that crystallinity can affect the T_g. In fact, Koleske *et al.* showed that the T_g of PCL was raised by crystallinity (ref. 7). The values of $\tan \delta$ at α peak are plotted in Figure 7. The decrease in the peak value of $\tan \delta$ with draw ratio corresponds to an increase in crystallinity.
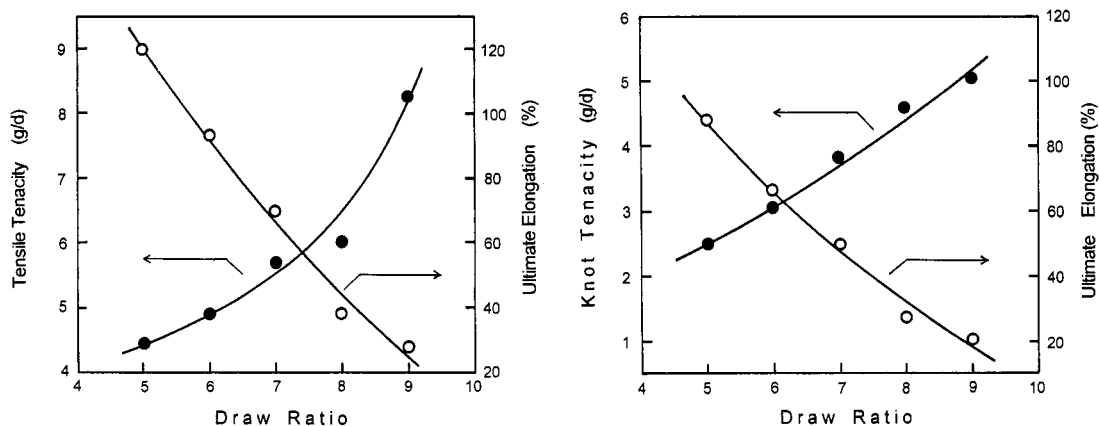

Fig. 4. Relationship between yarn properties and draw ratio :
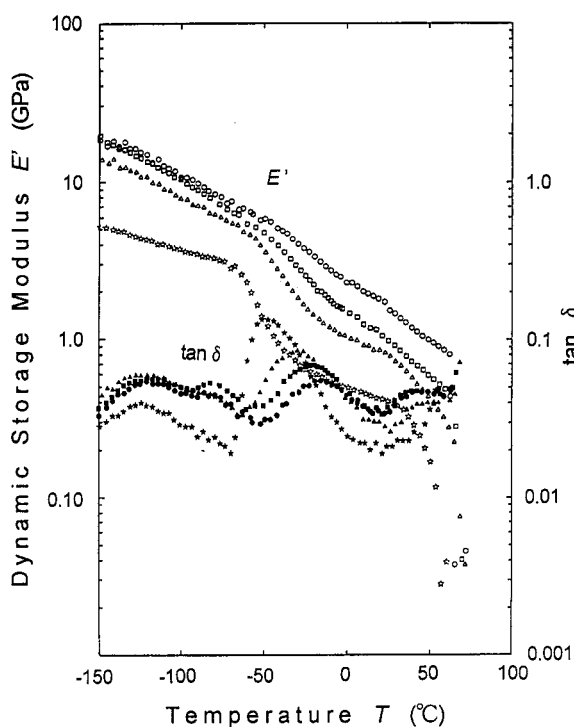(a) tensile properties, (b) knot properties.

Fig. 5. Temperature dependence of dynamic storage modulus and loss tangent ($tan\,\delta$) for undrawn and drawn PCL fibers at 3.5 Hz : ☆ undrawn PCL, △ DR=5, □ DR=7, ○ DR=9.

As is seen in Figure 5, stepwise decreases of the dynamic storage modulus (E') with temperature for undrawn and drawn fibers are observed in the glass transition regions. The behavior is marked for the undrawn fiber as compared with the highly drawn fibers. E' increases with the increase in draw ratio. The results are summarized in Figure 8, as the changes of E' with draw ratio at -150 and $23\,°C$.

In order to investigate the effect of molecular orientation on fiber stiffness, measurements of sonic pulse propagation along the fiber were performed at frequencies in the kHz range. The velocity of the longitudinal wave, C, was determined by measuring the transit time of a sonic pulse propagating along the length of fiber. The sonic modulus (E_s) was calculated using the equation,
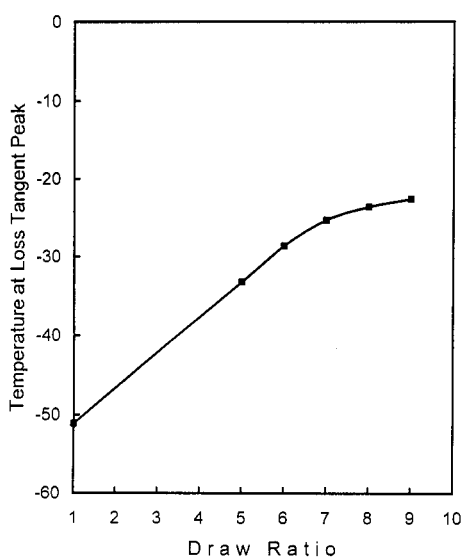

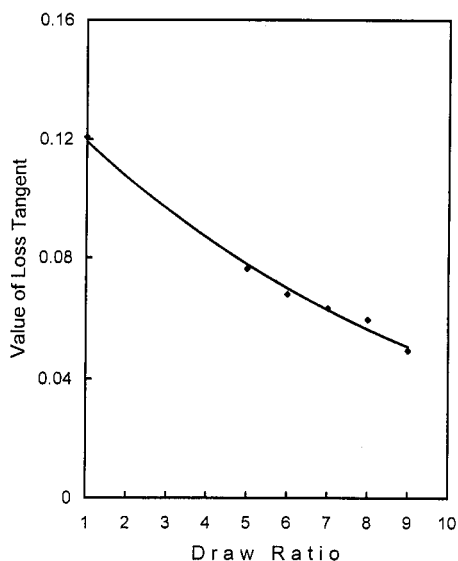Fig. 6. Temperature at $tan\,\delta$ peak (α dispersion) at 3.5 Hz vs. draw ratio.

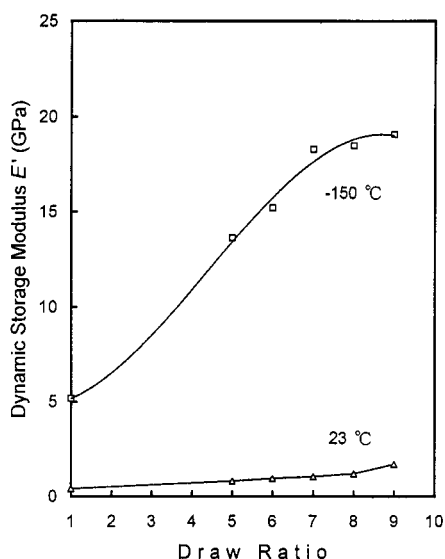Fig. 7. Loss $tangent\,\delta$ at α dispersion peak vs. draw ratio.

Fig. 8. Dynamic storage modulus E' vs. draw ratio : $\square$ $-150°C$, $\triangle$ $23°C$.
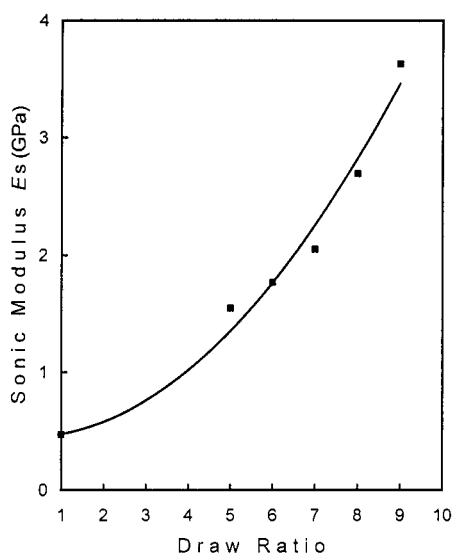

Fig. 9. Sonic modulus E_s vs. draw ratio.

$$E_s = \rho C^2 \qquad (1)$$

where ρ is the density of fiber.

Figure 9 shows that E_s increases with increase in draw ratio. The rapid increase in modulus for highly drawn fibers is due to the increase in the crystallinity and molecular orientation.

Figure 10 shows the dynamic moduli of undrawn and drawn PCL fibers as functions of frequency. The change of the modulus of the undrawn fiber with frequency was small, and the modulus for the drawn fibers increases largely, especially in the high frequency region. These results reflect the change of glass transition temperature with drawing and also structural characteristics or fine-structure of oriented fibers.
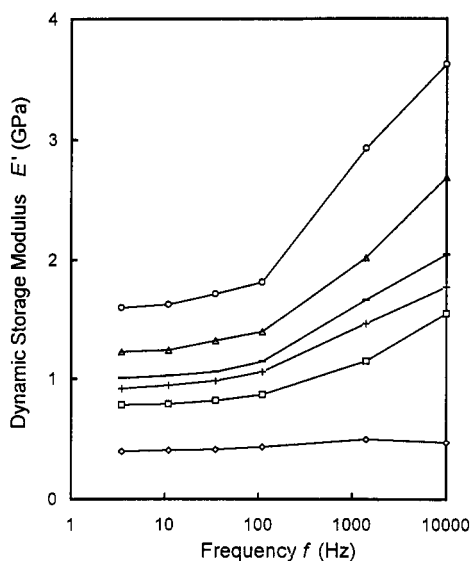

Fig. 10. Dynamic modulus E' vs. frequency : $\Diamond$ undrawn PCL, $\square$ DR=5, $+$ DR=6, $-$ DR=7, $\triangle$ DR=8, $\bigcirc$ DR=9.

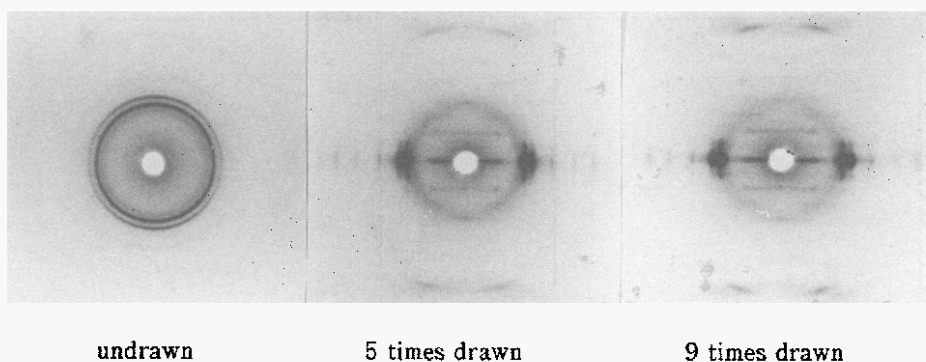undrawn   5 times drawn   9 times drawn

Fig. 11. X-ray diffraction patterns of undrawn and drawn PCL fibers.

Microstructure and molecular-chain orientation

As PCL is a semi-crystalline aliphatic polyester, changes in crystallinity, orientation and morphology may occur in the spin-draw process. It has been reported that the fine-structure of PCL influences the biodegradability of fibers and films (ref. 8,9,10,11). Therefore it is important to know the development of fine-structure during the spin-draw process. The unit cell of PCL was already determined as an orthorhombic structure by Chatani *et al.* (ref. 12) and also by Bittiger *et al.* (ref. 13).

Figure 11 shows wide-angle X-ray diffraction (WAXD) photographs of undrawn and drawn fibers. WAXD patterns of the drawn fibers exhibit typical c-axis orientation with clearly aligned reflections. The undrawn fiber shows only slight orientation. The (002), (004), (006), and (0014) reflections are observed in the intensity distribution curves of the drawn fibers, taking maxima on the meridian. The effect of drawing on the molecular orientation is very significant.

As reflections are clear and sharp, the crystallinity of drawn fibers should be fairly high. The crystallinity of PCL fibers evaluated by the Ruland method and the degree of orientation evaluated by the Hermans orientation function are shown in Table 2. Crystallinity index of an undrawn fiber was 40.0%. The crystallinity increased with the increase in draw ratio, reaching 69.3% at DR=9. The increase in crystallinity with drawing of PCL fiber is supported by increases in density and heat of fusion.

It is important to consider the molecular-chain orientation developed in drawn PCL fibers. Figure 12 shows the degree of orientation (*f*) of PCL fibers plotted against draw ratio. The crystalline c-axis orientation function (f_c) was evaluated by an X-ray diffraction method. Hermans orientation function was calculated from the following equation by use of azimuthal intensity distribution, $I(\phi_{006})$, of (006).

$$f_c = (3 \langle \cos^2 \phi_{006} \rangle - 1)/2 \qquad (2)$$

Moseley has proposed a semi-empirical equation to relate the sonic velocity to orientation (ref. 14):

$$f_s = 1 - E_u/E_s \qquad (3)$$

where E_u and E_s are the sonic moduli for an unoriented sample and oriented samples, respectively. In this case, f_s shows the degree of orientation over the average of crystalline and amorphous phases.

The results calculated for drawn PCL fibers are also shown in Figure 12. Comparing f_c with f_s, it is seen that the crystallites of PCL are more highly oriented, and approach higher degree of orientation at lower draw ratio, than the amorphous phase.
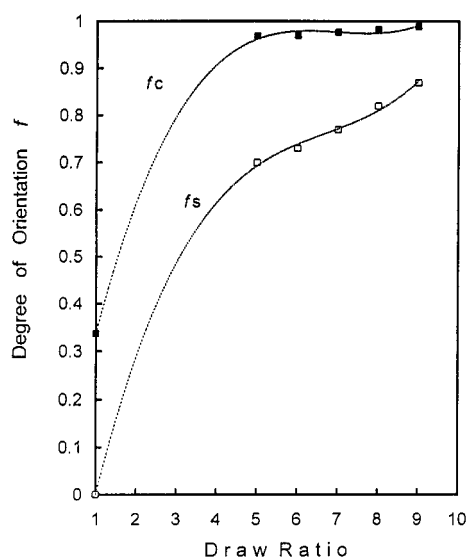
Fig. 12. Degree of orientation f vs. draw ratio : f_c calculated as Hermans orientation function from azimuthal distribution of (006), f_s calculated by sonic modulus.

CONCLUSIONS

Tough and high tenacity poly(ϵ -caprolactone) fibers were obtained by melt-spinning with subsequent drawing. Thermal, mechanical, and thermomechanical properties of the fibers were significantly affected by drawing which advanced c-axis orientation with an icrease in crystallinity. The molecular orientation with the increase in crystallinity accounts for the change in thermal properties such as increases in melting temperature, heat of fusion, glass transition temperature, and *tan δ* peak value, as well as the change in mechanical properties such as increases in tensile tenacity, knot tenacity, dynamic storage modulus, and sonic modulus with draw ratio.

REFERENCES

1. M. Mochizuki and M. Hirami, in "Polymers and Other Advanced Materials", P. N. Prasad, E. Mark, and T. J. Fai, eds., Plenum Press, New York (1995), p.589
2. G. L . Brode and J. V. Koleske, J. Macromol. Sci., Chem., 6(6), 1109 (1972)
3. Union Carbide Corporation, Bound Brook NJ, Product Brochure for Tone Polymers
4. W. Ruland, Acta Cryst., 14, 1180 (1961)
5. P. H. Hermans, in "Physics and Chemistry of Cellulose Fibers", Elsevier, New York (1949), p.244
6. R. S. Stein, J. Polym. Sci., 31, 327 (1958)
7. J. V. Koleske and R. D. Lundberg, J. Polym. Sci. A-2, 7, 795 (1969)
8. W. J. Cook, J. A. Cameron, J. P. Bell, and S. J. Huang, J. Polym. Sci., Polym. Lett. Ed., 19, 159 (1981)
9. P. Jar, S. J. Huang, J. P. Bell, J. A. Cameron, and C. Benedict, Org. Coat. Appl. Polym. Sci. Proc., 47, 45 (1982)
10. C. V. Benedict, W. J. Cook, P. Jarrett, J. A. Cameron, S. J. Huang, and J. P. Bell, J. Appl. Polym. Sci., 28, 327 (1983)
11. M. Mochizuki, M. Hirano, Y. Kanmuri, K. Kudo and Y. Tokiwa, J. Appl. Polym. Sci., 55, 289 (1995)
12. Y. Chatani, Y. Okita, H. Tadokoro, and Y. Yamashita, Polymer J., 1(5), 555 (1970)
13. H. Bittiger, R. H. Marchessault, and W. D. Niegish, Acta Crystallogr., B26, 1923 (1970)
14. W. W. Moseley, Jr., J. Appl. Polym. Sci., 3(9), 266 (1960)